# Effect of the Surface State of Steel on the Microstructure and Mechanical Properties of Dissimilar Metal Lap Joints of Aluminum and Steel by Friction Stir Welding

Y.C. CHEN and K. NAKATA

Friction stir lap joints of AC4C Al alloy (top sheet) and steel (zinc-coated steel, brushed finish steel, and mirror finish steel) were produced when the friction stir welding tool did not touch the lower steel surface. For zinc coat steel, the strength of joints could reach 97.7 pct of that of steel; for brushed finish steel, the strength was 63.2 pct of that of steel; for mirror finish steel, Al alloy and steel could not be welded. The effect of the surface state of steel on the microstructure and mechanical properties of dissimilar metal friction stir lap joints of AC4C Al alloy and steel was discussed.

DOI: 10.1007/s11661-008-9523-4


## I. INTRODUCTION

As a solid-state welding technology, friction stir welding (FSW) process[1] can join Al alloys and steels and get higher quality joints than fusion welding technology. It is also possible that good welds can be produced when FSW is used to join dissimilar materials.[2–18] The need of light weight in automotive body construction leads to the increasing use of the lap joining of aluminum alloy and steel in the fabrication of vehicles.[19,20] Therefore, the development of reliable joints between aluminum alloy and steel is required.

Elrefaey *et al.* studied the feasibility of friction stir lap welding (FSLW) a commercially pure aluminum plate to a low-carbon steel plate and investigated the effects of welding parameters on joint strength.[14] It was reported that joint strength depended on the depth of the probe tip into the steel surface. When the probe tip did not reach the steel surface, the joint failed under low applied loads. However, slight penetration of the probe tip to the steel surface significantly increased joint strength. Kimapong and Watanabe reported the results about FSLW of 5083 aluminum and SS400 steel.[15,16] They showed that the joint shear strength decreased with an increasing tool tilt angle and a probe diameter due to the formation of a thick Al5Fe intermetallic compound layer at the joint interface. The weld quality of FSLW of aluminum and steel was difficult to control because of the formation of some intermetallic compounds at the weld interface. However, some recent attempts at joining aluminum and zinc-coated steel using FSLW turned out to be successful.[17,18] The adoption of zinc-coated steel evidently improved the friction stir weldability of aluminum and steel and made the full-strength joints possible. Chen *et al.* investigated the FSLW feasibility of AC4C cast aluminum alloy and low-carbon zinc-coated steel.[17] They reported that welding speeds had a significant effect on the tensile properties and fracture locations of the joints. With appropriate welding parameters, full-strength joints could be obtained and joints fractured at the zinc-coated steel base material side. Elrefaey *et al.* investigated the weldability of 1100H24 Al alloy and zinc-coated steel using FSLW.[18] They found that the Al/zinc-coated steel joint exhibited considerable fracture load, while Al/steel joints were so weak that they fractured at the same probe depth during preparation of the specimen for metallographic analysis.

Current reporting literature distinctly shows that the surface state of steel has a significant effect on the weldability of Al and steel in friction stir lap joints. So far, systematic research about the effect of the surface state of steel on the weldability of Al alloy and steel in friction stir lap joints has not been reported. Studies on this topic are important for us to reveal the friction stir weldability of Al alloy and steel.

In this study, 3-mm-thick AC4C cast aluminum alloy and three types of 0.8-mm-thick steel sheets (zinc-coated steel, brushed finish steel, and mirror finish steel) are selected as the experimental materials for friction stir lap welding. The aluminum alloy sheet is put on the steel sheet. In order to eliminate the effect of the insert depth of the tool and to highlight the effect of the surface state of steel on the weldability, a 2.8-mm-length probe is selected. That is, the probe tip of the tool does not touch the surface of the steel sheet during welding. The present study examines the tensile properties of joints and microstructural features in the lap interface and discusses the effect of the surface state of steel on the weldability of Al alloy and steel in friction stir lap joints.

## II. EXPERIMENTAL PROCEDURE

The base materials used in this study were a 3-mm-thick AC4C cast aluminum alloy sheet and a 0.8-mm-thick

Y.C. CHEN, Researcher, and K. NAKATA, Professor, are with the Joining and Welding Research Institute, Osaka University, Ibaraki, Osaka 567-0047, Japan. Contact e-mail: armstrong@hit.edu.cn

Manuscript submitted October 21, 2007.
Article published online May 17, 2008

low-carbon steel sheet. For comparison, three kinds of steel sheets were selected, *i.e.*, zinc-coated steel, brushed finish steel, and mirror finish steel. The chemical composition and mechanical properties of the base materials are shown in Table I. Rectangular welding samples, 300-mm long by 100-mm wide, were lap welded using an FSW machine. The welding parameters are rotation speed of 800 rpm and welding speed of 80 mm/min. The upsetting force of the welding tool (made of SKD61 steel) is 5.88 kN. The shoulder diameter and probe diameter of the tool are 15 and 5 mm, respectively. The length of the probe is 2.8 mm, and the welding tilt angle is 3 deg.

After welding, the joint was cross sectioned perpendicular to the welding direction for the metallographic analysis and tensile tests using an electrical-discharge cutting machine. The cross sections of the metallographic specimens were polished with a diamond polishing agent, etched with Keller's reagent (1 mL hydrochloric acid, 1.5 mL nitric acid, 2.5 mL hydrofluoric acid, and 95 mL water), and observed by optical microscopy. The mechanical properties of the joint were measured using tensile tests. The tensile tests were carried out at room temperature at a crosshead speed of 1 mm/min using a tensile testing machine, and the mechanical properties of the joint were evaluated using three tensile specimens cut from the same joint. The shape of the test specimen is rectangular, and the width of each specimen is 20 mm.

The welding thermal cycle histories along the interface during FSW were measured with an array of K-type thermocouples (0.2-mm diameter) at various locations from the weld center. Microstructure characteristic and element distribution along the interface were analyzed by scanning electron microscopy (SEM) equipped with an energy-dispersive X-ray spectroscopy (EDS) analysis system. The fracture surfaces of joints were analyzed using X-ray diffraction (XRD) after the tensile test.

## III. EXPERIMENTAL RESULTS

Table II shows the tensile strengths and fracture locations of lap joints of AC4C aluminum and three kinds of steels. Tensile test results show that the surface state of steel has a significant effect on the mechanical properties of lap joints welded at the same welding parameters. For zinc-coated steel, the failure load of joints can reach 5.02 kN, which is equal to 97.7 pct of that of the steel base metal. The joints fracture at the interface. For brushed finish steel, the failure load of joints is equal to 63.2 pct of that of the steel base metal. The joints fracture at the interface. For mirror finish steel, the joints split during preparing the tensile test samples. These results indicate that the presence of zinc coat greatly improves the friction stir lap weldability of aluminum and steel.

**Table II. Tensile Test Results**

| Joint Type | Failure Force | Fracture Location |
|---|---|---|
| Steel sheet base metal | 5.14 kN* | — |
| Zinc-coated steel joints | 5.02 kN | interface |
| Brushed finish steel joints | 3.25 kN | interface |
| Mirror finish steel joints | — | — |

*The width of the base material is 20 mm.

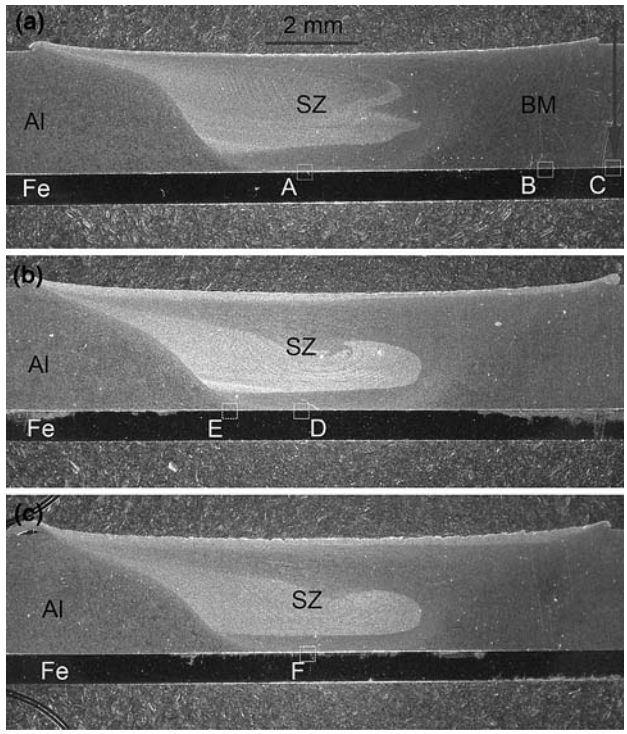


Fig. 1—Cross sections of (*a*) zinc-coated steel joint, (*b*) brushed finish steel joint, and (*c*) mirror finish steel joint. Rectangular areas A through F indicate the position of the microstructural observation.

The macroscopic views of traverse sections of three kinds of joints are shown in Figure 1. It can be seen that aluminum and steel are joined tightly, and the microstructure characteristic in the aluminum side is similar to that of the friction stir-welded aluminum alloy. In this case, we are mainly interested in the structural features of the interface. Microstructure is observed in the region from the center of the weld to the base material. The typical details of the microstructural variations from

**Table I. Chemical Composition and Mechanical Properties of Base Materials**

| | Chemical Compositions (Mass Pct) | | | | | | | | | | Mechanical Properties | |
|---|---|---|---|---|---|---|---|---|---|---|---|---|
| Base Materials | Al | Cu | Mn | Fe | C | Mg | Ni | P | Si | S | Strength (MPa) | Elongation (Pct) |
| AC4C | bal | 0.05 | 0.3 | 0.15 | — | 0.2 | — | — | 7.5 | — | 244 | 7.4 |
| Steel | 0.06 | 0.02 | 0.20 | bal | 0.04 | — | 0.01 | 0.013 | — | 0.005 | 328 | 33.4 |

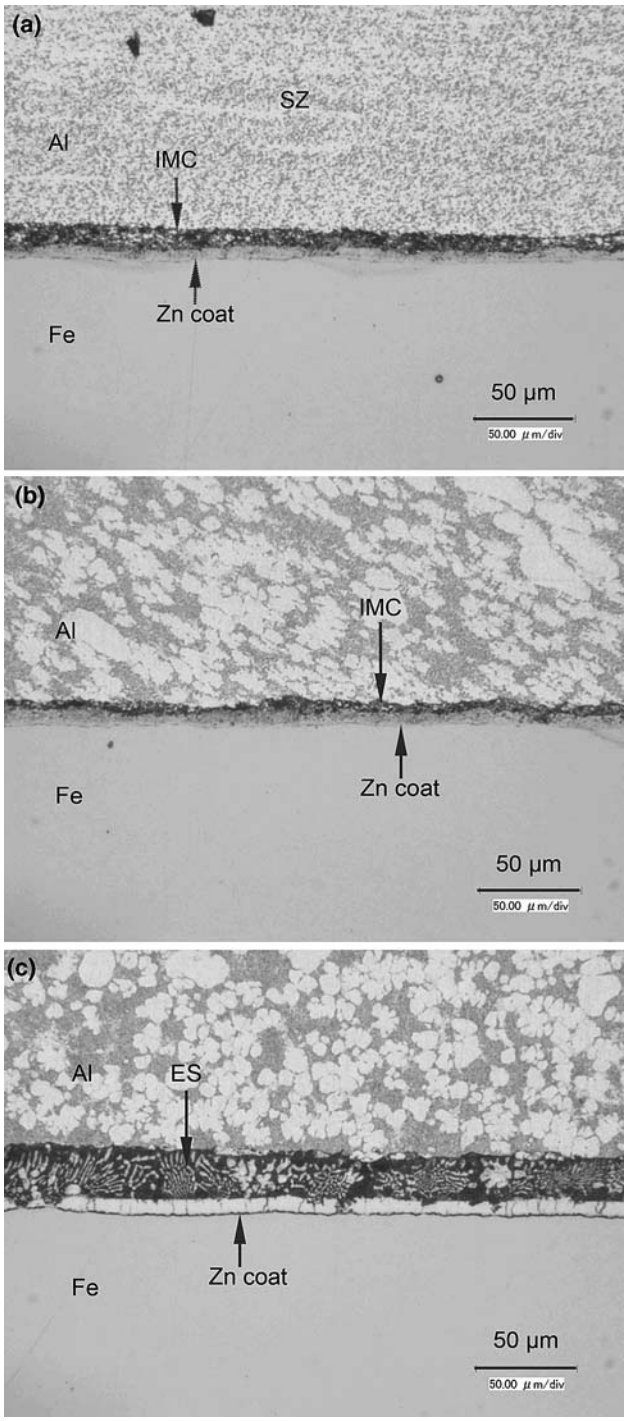


Fig. 2—Microstructure in the joints shown in Fig. 1 from position A to position C: (*a*) position A, (*b*) position B, and (*c*) position C.

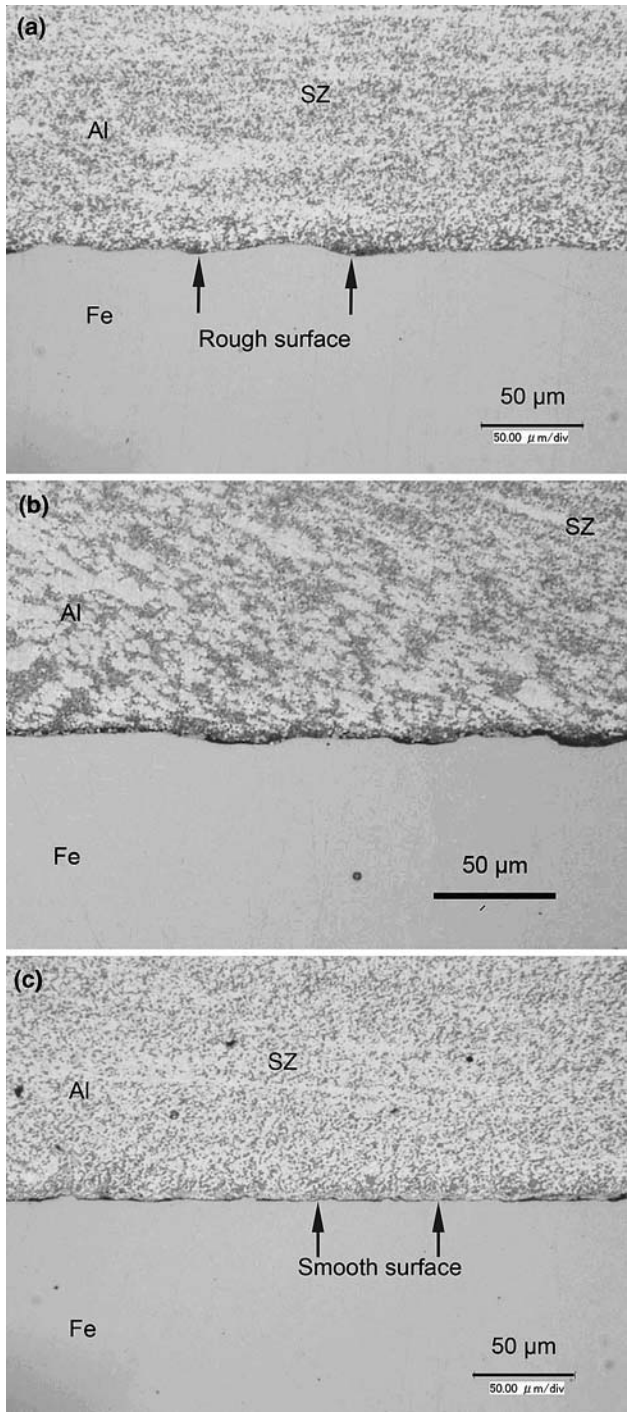


Fig. 3—Microstructure in the joints shown in Fig. 1 from position D to position F: (*a*) position D, (*b*) position E, and (*c*) position F.

position A to position F are demonstrated in Figures 2 and 3.

Figure 2 shows microstructural variations at the lap interface of aluminum and zinc-coated steel. It can be seen from Figure 2(a) that the joint consists of a four-layer structure, *i.e.*, microstructure in the stir zone (SZ) of aluminum alloy, a new intermetallic compound (IMC) layer, a residual zinc layer, and the base metal of steel. Aluminum alloy and steel are joined through the intermediate reaction zone. Figure 2(b) shows the microstructure of the B region shown in Figure 1(a). This region is far from the SZ but still under the shoulder. The four-layer structure mentioned previously is still present. Figure 2(c) shows the microstructure of the C region shown in Figure 1(a). From this position, aluminum alloy and zinc-coated steel are in unbound state. A typical eutectic structure (ES) is found. The ES fills into the clearance between aluminum alloy and

zinc-coated steel. As shown in Figure 1(a), this position has slightly exceeded the domain of shoulder diameter of the tool. In the current experimental condition, the ES region locates at the position of 8 mm from the weld center.

Figures 3(a) and (b) show microstructural variations at the lap interface of aluminum and brushed finish steel. It can be seen from Figure 3(a) that no significant IMC layer was found at the interface in SZ. Aluminum metal is pushed into the concavities of the brushed finish steel surface. Aluminum alloy and steel are joined through some kind of mechanical joining, and the joining region is only under the domain of the probe diameter (Figure 3(b)). However, AC4C aluminum and mirror finish steel cannot be welded at the same parameters. Aluminum and mirror finish steel split during preparing the metallographic sample. Figure 3(c) shows the smooth surface of the mirror finish steel.

The representative concentration profiles of Al, Si, Zn, and Fe that cross the interface at different positions (positions A, C, and D shown in Figure 1) between aluminum alloy and steel are shown in Figures 4 through 6. For zinc-coated steel joints, a layer involving Al, Fe, Zn, and Si is formed at the interface of the joint in position A. The following XRD results show that a new IMC layer is produced at the interface; results from position C show that the concentration profiles of Al and Zn are detected in the ES layer, which indicates that this region is an Al-Zn eutectic structure region. For brushed finish steel joints, no significant concentration

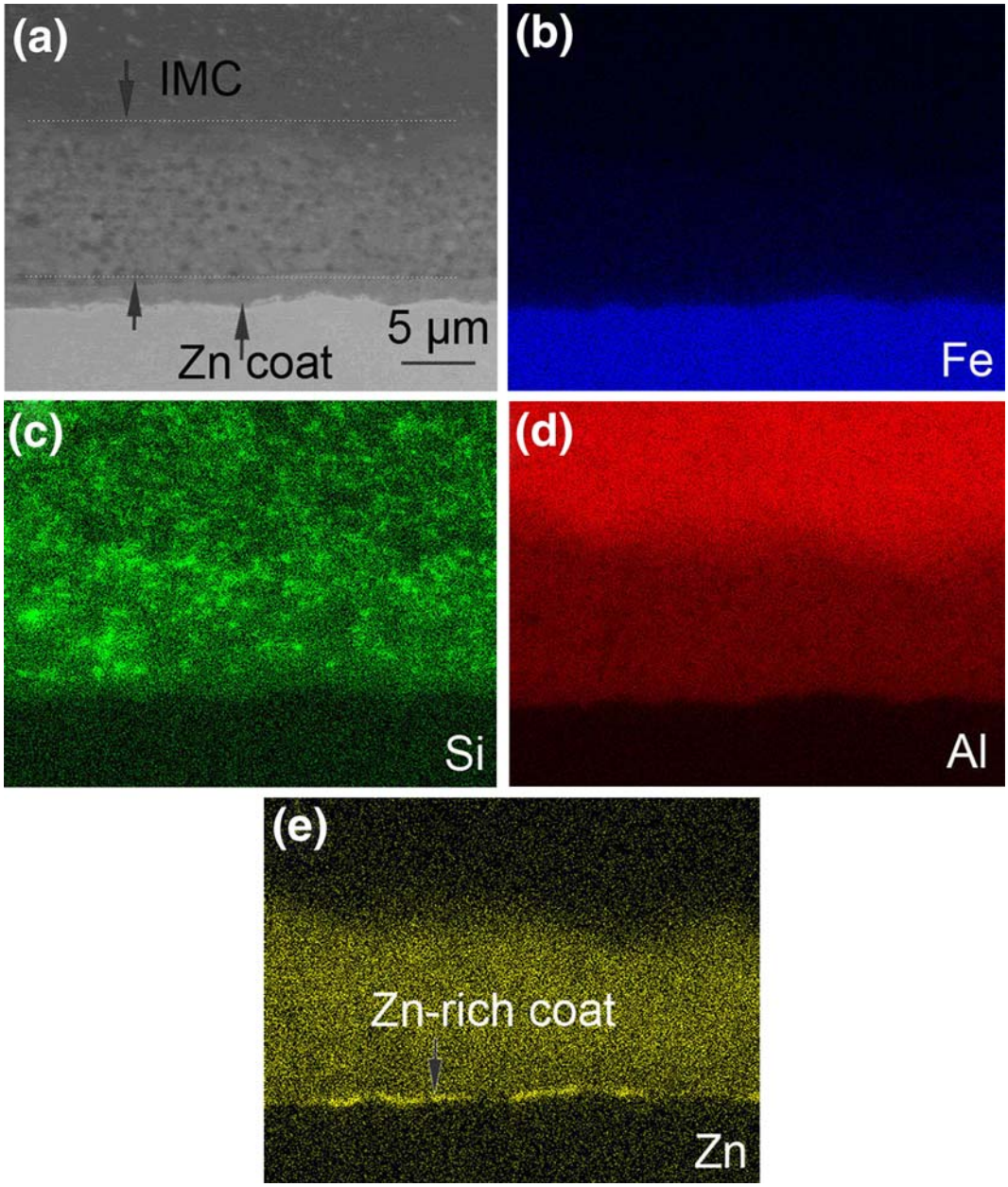


Fig. 4—SEM and EDS analysis results of position A shown in Fig. 1.

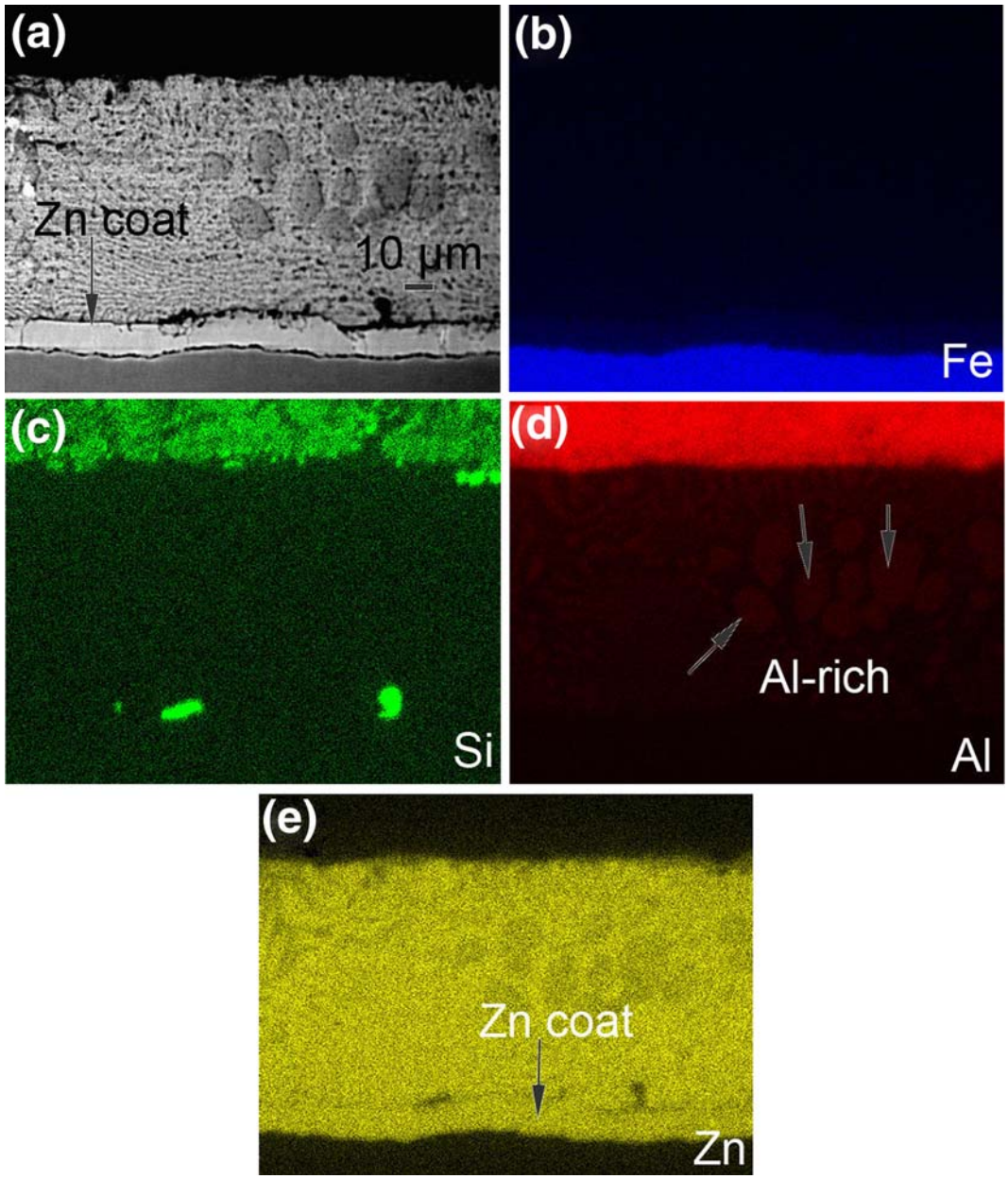


Fig. 5—SEM and EDS analysis results of position C shown in Fig. 1.

profiles of elements are detected at the interface (position D), suggesting that no new IMC layer is produced during welding.

In order to determine whether intermetallic compounds are formed at the interface, X-ray diffraction patterns from fractured surfaces of the aluminum and steel sides are analyzed. The XRD analysis results from the fractures are shown in Figure 7. For zinc-coated steel joints, diffraction lines that are attributable to intermetallic compounds of Fe2Al5 and Fe4Al13 are detected at the aluminum side and steel side. At the same time, elements of Si, Al, and Fe are also found. This discovery means that the new IMC layer mainly contains intermetallic compounds of Fe2Al5 and Fe4Al13. For brushed finish steel joints, only elements of Si, Al, and Fe are detected. This result shows that no IMC layer is produced at the interface when the brushed finish steel is selected as the base metal. The joining mechanism between aluminum and brushed finish steel is mechanical joining.

To further clarify the joining mechanism, welding heat cycle histories are measured with an array of K-type thermocouples during welding, as shown in Figure 8. It is notable from the preceding interface structure analysis results that the position of 8 mm is the location of ES when zinc-coated steel is selected as the base metal. The peak temperatures are shown in Table III. The peak temperatures in the interface center are 455 °C to 479 °C. Such temperature range is lower than the melting points of the Al and Fe base metal (660 °C and 1538 °C, respectively), but higher than those of the Zn melting point and Al-Zn eutectic point

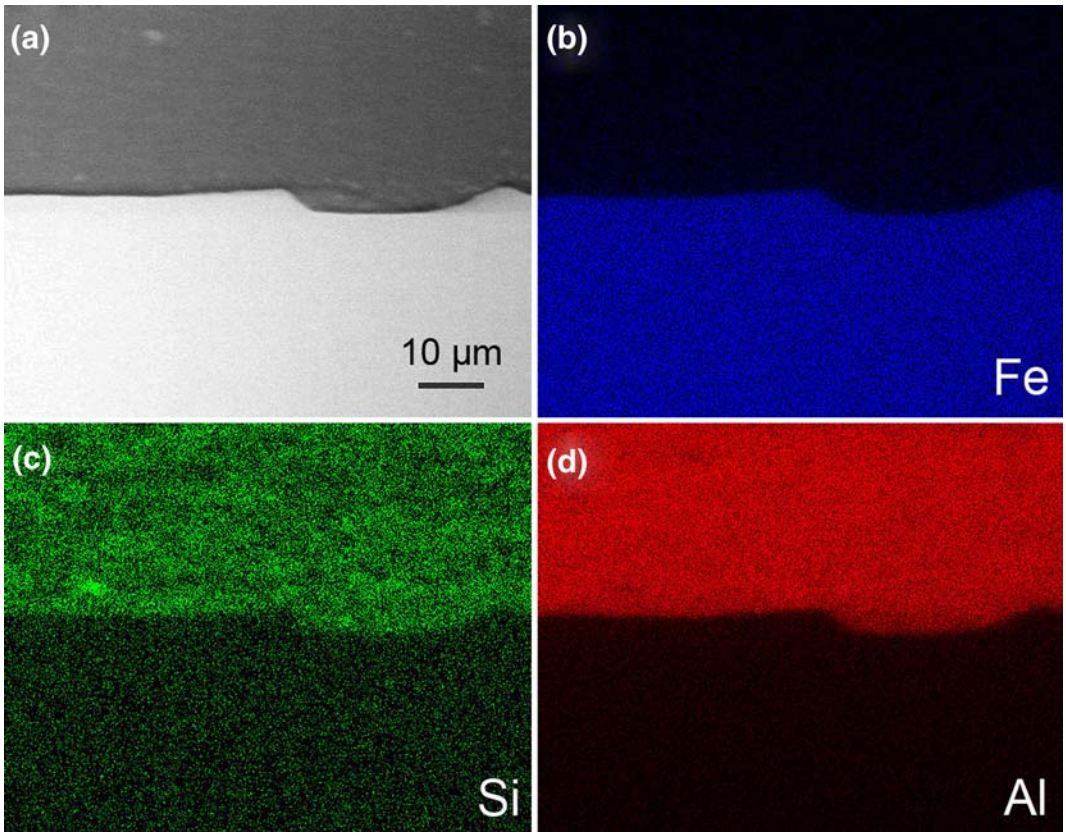


Fig. 6—SEM and EDS analysis results of position D shown in Fig. 1.

(420 °C and 381 °C, respectively).[21] Moreover, the peak temperature in the position of 8 mm is 385 °C (zinc-coated steel), which is almost the same as the eutectic temperature of Al-Zn. This finding means that the liquid Al-Zn eutectic structure can be formed because of a high peak temperature at the center interface and can be pushed aside. From the viewpoint of peak temperature, the eutectic structure can reach the position of 8 mm in the current welding condition.

## IV. DISCUSSION

Microstructure analysis and mechanical property test results show that the surface state of steel has a significant effect on the friction stir lap weldability of Al alloy and steel. For the solid-state bonded joint of dissimilar metals, there are two main factors controlling the joining performance.[22] One is the intimate contact between aluminum and steel, and the other is the microstructure, particularly the formation of intermetallic compounds. In our experiment, the surface of steel does not receive any surface treatment before welding in order to focus on the effect of the original surface state of steel on weldability. No fresh metal surface is exposed before welding so that there is no intimate contact between aluminum and steel. Therefore, Al/mirror finish steel and Al/brushed finish steel joints will not exhibit considerable fracture load. For brushed finish steel, there are lots of concavities on the rough surface and large deformation aluminum metal is pushed into these concavities during welding. Aluminum alloy and steel are joined through mechanical joining, and the joining region is only under the domain of the probe diameter. For mirror finish steel, the steel surface is quite smooth and the joint cannot be successfully produced even through the mechanical joint method. The joint is so weak that it fractures during preparation of the specimen for metallography. However, for zinc-coated steel, the joint exhibits considerable failure load compared with the two kinds of no-zinc-coat steel joints. Obviously, the presence of zinc coat significantly improves the weldability of aluminum and steel.

It should be pointed out that the zinc-coated steel is produced using a hot-dip galvanizing process. Therefore, actually, the zinc coat on the surface of steel is composed of iron-zinc intermetallic compounds. The zinc coat firmly joins with steel through iron-zinc intermetallic compounds, but its surface composition approaches pure zinc.[23]

During friction stir welding, the metal in the lap interface undergoes the synthetic effect of the thermal cycle and the mechanical cycle because of the action of friction, stir, and extrusion of the tool. Thus, high temperature and high pressure are generated at the interface. High temperature first leads to the melting of pure zinc on the surface of the zinc coat, and high pressure simultaneously results in the rupture of surface

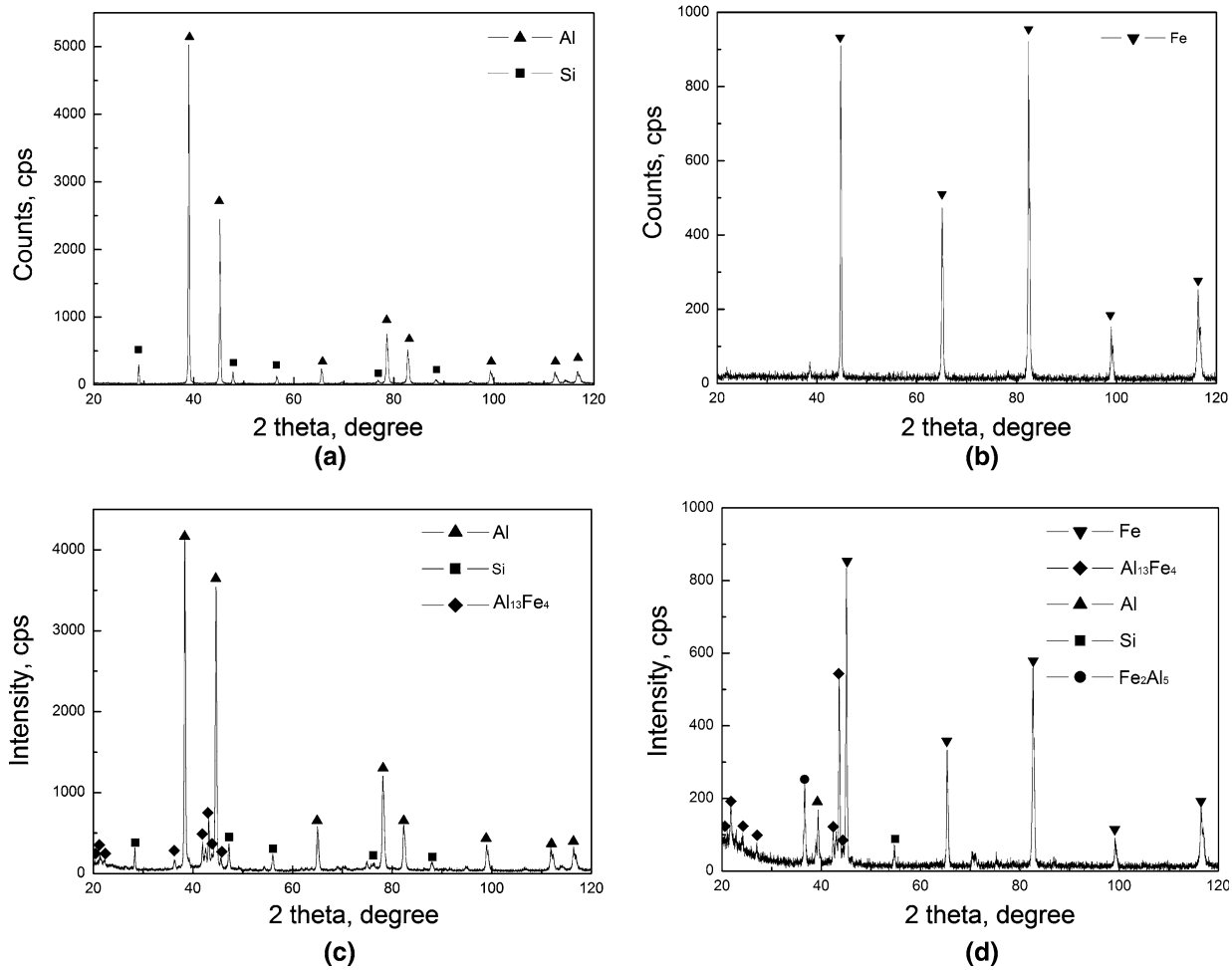


Fig. 7—XRD analysis results from the fracture surface of joints: (*a*) Al side of a brushed finish steel joint, (*b*) Fe side of a brushed finish steel joint, (*c*) Al side of a zinc-coated steel joint, and (*d*) Fe side of a zinc-coated steel joint.

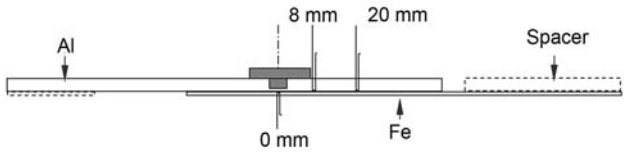


Fig. 8—Locations of inserted thermocouples for temperature measurement during FSW.

**Table III. Peak Temperatures at Different Locations**

| Joint Type | 0-mm Location | 8-mm Location | 20-mm Location |
|---|---|---|---|
| Zinc coat steel joint | 471 °C | 385 °C | 197 °C |
| Brushed finish steel joint | 455 °C | 371 °C | 202 °C |
| Mirror finish steel joint | 479 °C | 379 °C | 218 °C |

oxide films at both sheet surfaces, which promotes the formation of low-melting Al-Zn eutectic reaction products. High pressure extrudes the liquid phase of Al-Zn eutectic reaction product with broken oxide films and surface contamination far from the weld center, which spreads along the interface until it piles into the natural clearance between two sheets. The final position of the liquid Al-Zn eutectic phase can reach near the position of the edge of the shoulder, where the peak temperature is almost the same as the Al-Zn eutectic temperature. In this way, the fresh interfaces of Al and the residual zinc layer are exposed, and they are tightly extruded together after the liquid eutectic phase is pushed out. Mutual diffusion of aluminum and iron occurs in elements, which leads to the formation of a new intermetallic compound layer adjacent to the lap interface of the weld. Finally, during cooling after welding, liquid Al-Zn eutectic phase transforms to solid eutectic structure.

## V. CONCLUSIONS

AC4C aluminum alloy and three kinds of steels were lap welded using friction stir welding technology. The effect of the steel surface state on the weldability of aluminum and steel was investigated.

The AC4C/zinc-coated steel joint showed higher fracture strength than the AC4C/brushed finish steel and AC4C/mirror finish steel joints, suggesting that the

presence of zinc coat significantly improved the weldability of aluminum and steel. From the viewpoint of microstructure, the appearance and extrusion of low-melting eutectic phase at the interface led to the exposure of fresh metal surface and increased the mutual diffusion degree between aluminum and steel.

## REFERENCES


1. C.J. Dawes and W.M. Thomas: *Weld. J.*, 1996, vol. 75, pp. 41–45.
2. T. Watanabe, H. Takayama, and A. Yanagisawa: *J. Mater. Proc. Technol.*, 2006, vol. 178, pp. 342–49.
3. T. Watanabe, H. Takayama, K. Kimapong, and N. Hotta: *Mater. Sci. Forum.*, 2003, vols. 426–432, pp. 4129–34.
4. T. Watanabe, H. Takayama, A. Yanagisawa, and S. Konuma: *Q. J. Jpn. Weld. Soc.*, 2005, vol. 23, pp. 603–07.
5. W.H. Jiang and R. Kovacevic: *Proc. I. Mech. E, Part B: J. Eng. Manufacture*, 2004, vol. 218, pp. 1323–31.
6. U. Huseyin, D.D. Claudio, A. Alberto, G. Tommaso, and G. Carla: *Mater. Design*, 2005, vol. 26, pp. 41–46.
7. T. Yasui, Y. Shimoda, M. Tsubaki, T. Ishii, and M. Fukumoto: *Q. J. Jpn. Weld. Soc.*, 2005, vol. 23, pp. 469–75.
8. T. Yasui, Y. Shimoda, M. Tsubaki, and M. Fukumoto: *Mater. Sci. Forum.*, 2004, vols. 449–452, pp. 433–36.
9. K. Kimapong and T. Watanabe: *Weld. J.*, 2004, vol. 83, pp. 277–82.
10. C.M. Chen and R. Kovacevic: *Int. J. Mach. Tool. Manufact.*, 2004, vol. 44, pp. 1205–14.
11. W.B. Lee, M. Schmuecker, U.A. Mercardo, G. Biallas, and S.B. Jung: *Scripta Mater.*, 2006, vol. 55, pp. 355–58.
12. K. Tanaka, M. Kumagai, and H. Yoshida: *J. Jpn. Inst. Light Met.*, 2006, vol. 56, pp. 317–22.
13. J. Barnes: *Adv. Mater. Proc.*, 2005, vol. 163, p. 29.
14. A. Elrefaey, M. Gouda, M. Takahashi, and K. Ikeuchi: *J. Mater. Eng. Perf.*, 2005, vol. 14, pp. 10–17.
15. K. Kimapong and T. Watanabe: *Mater. Trans.*, 2005, vol. 46, pp. 2211–17.
16. K. Kimapong and T. Watanabe: *Mater. Trans.*, 2005, vol. 46, pp. 835–41.
17. Y.C. Chen, T. Komazaki, Y.G. Kim, T. Tsumura, and K. Nakata: *Int. Welding and Joining Conf.*, Seoul, Korea, 2007, pp. 435–36.
18. A. Elrefaey, M. Takahashi, and K. Ikeuchi: *Q. J. Jpn. Weld. Soc*, 2005, vol. 23, pp. 186–93.
19. G. Kobe: *Chilton's Automotive Industries*, 1994, vol. 174, p. 44.
20. S. Ramasamy: *Weld. J.*, 2000, vol. 79, pp. 35–39.
21. *Alloy Phase Diagrams*, vol. 3, *ASM Handbook*, ASM, Materials Park, OH, 1993, pp. 2.44–2.56.
22. K. Kobayashi, K. Nishimoto, and K. Ikeuchi: *Introduction to Joining Engineering of Materials*, Sampo, Tokyo, 2002, pp. 182–88.
23. A.R. Marder: *Progr. Mater. Sci.*, 2000, vol. 45, pp. 191–271.